Available online www.ejaet.com

European Journal of Advances in Engineering and Technology, 2024, 11(11):7-27

Research Article ISSN: 2394 - 658X

A pipelined, multilayer AI model for point-of-care diagnosis of spinal cord disorders using clinical dataset

Kumari Bhawana

PhD Scholar,
Computer Science and Engineering,
BIT Mesra, Ranchi, Jharkhand, India

ABSTRACT

Back pain poses a significant health, social, and economic burden, making early detection of spinal cord disorders essential through point-of-care technology (POCT). Numerous techniques have been developed to detect spinal disorders, yet issues persist due to labeling inaccuracies and segmentation errors from missed vertebrae, leading to improper classification. To address these challenges, a novel approach named the Pipelined Multilayer AI-based Point-of-Care Model for Spinal Cord Disorder Diagnosis in Large Clinical Data is proposed, enabling effective spinal disorder detection. This model employs Pipelined Labeling with Level Count Circular Localization, utilizing a pipelined stochastic convolutional labeling neural network (NN) that distinctly labels similar vertebrae. However, existing techniques struggle with localization errors in cases of anatomical anomalies, such as additional or transitional lumbar vertebrae. Thus, a Circular Anisotropic Localization Mechanism and Level Check Counter NN are incorporated to minimize localization errors and identify anatomical abnormalities. Additionally, current semantic and automated segmentation methods produce rough image details, often missing vertebrae and yielding low dice scores. To counter this, the proposed model uses a Multi-Atlas Instance SegNet to segment localized spinal components with a high dice score. Moreover, existing models typically recognize specific spinal disorders without extracting critical features, causing misclassification. To enhance detection, a Domineering Feature Transformer-based Classification method is introduced, employing a Visual Bipartite Matching Loss Feature Transformer to extract features and a Bilsky Phenotype Grading Classifier to boost detection accuracy without misclassification across various spinal disorders. Consequently, the proposed model achieves an effective detection rate with high true-positive (TP) rate and F-measure, recorded at 0.97% and 0.98%, respectively, while reducing error to 0.06% and runtime to 2100ms.

Keywords: Spinal cord disorder, Spondylolisthesis, spinal stenosis, POCT, Localized, misclassification,

---

INTRODUCTION

Point-of-care technology (POCT) enables quick clinical decision-making by providing actionable information at the point of care. POCT refers to the devices or services that are used to offer clinical decision support and give quick laboratory results in real time. The outcome from POC devices was uploaded to laptops that were used across the hospital. With the aid of that information, laboratories could determine the quality of clinical data and diagnose the diseases with better clinical decision making [1,2]. Hence, in order to enhancing the outcome in evaluating the potential of health care, a simple yet effective and scalable large data analysis system can be used. Artificial intelligence (AI) has been employed more frequently in diagnostics in recent years. AI may be easily included into POCT in clinical pathology to maintain the quality of big clinical data and to produce effective findings when interpreting diseases via automated diagnostic classifiers [3-5]. The most common reason for adult clinical visits in contemporary cultures is back pain, which is brought on by ailments including spondylolisthesis and spinal stenosis, incurring significant costs and reducing living quality and job performance [6]. Hence, it is necessary to diagnose the spinal cord disorders from large clinical scanned images at an early stage with point of care.

Machine learning (ML) and deep learning (DL) techniques are widely used in the prediction and diagnosis of spinal cord disorders that include spinal oncology, spinal osteoarthritis, trauma, infections, degenerative diseases, and

adult spinal deformity. Spinal osteoarthritis, Lumbar Spinal Stenosis (LSS) and spinal deformities are the leading cause for back pain [7,8]. Spinal osteoarthritis often known as non-inflammatory or degenerative arthritis develops over time and usually affects the lower back in whichinflammation and pain are caused by the gradual breakdown of the cartilage between the joints. Scoliosis is a three-dimensional deformation of the spine that affects a large portion of the population and is more common in women than in males. Because of this, it is considered catastrophic and should be diagnosed early to prevent major issues with the spinal intervertebral column. LSSis one of the major factors contributing to persistent lower back discomfort. It is a constriction of the lumbar spinal canal brought on by swelling of the soft tissues or bone, which puts pressure on the spinal nerve roots. Patients will experience symptoms like neurogenic claudication, radicular pain, and unusual leg pain. For predicting these spinal cord disorders with an early-stage alert, ML and DL techniques process large clinical dataset containing spinal radiography images, Computer tomography (CT) images and magnetic resonance imaging (MRI) imageswith effective segmentation and classification [9,11]. Segmentation of spinal cord images has been previously done with fuzzy c-means method (FCM) and other soft segmentation approaches. The quantification of disc degradation, computer-aided disease diagnosis, and computer-assisted spine surgery would all benefit from correct segmentation of intervertebral discs [12,13]. However, none of these studies provided quantitative segmentation accuracy evaluation results.

Automatic DL methods such as CNN, U-Net and DNN for spinal cord disorder detection on a large clinical CT, radiography and MRI images might notify the reporting radiologist and clinicians, enabling a speedy decision for confirmation and therapy planning of spinal cord disorders. By doing so, the need for medical resources would be lessened and earlier treatment might be given to prevent neurological impairment that is irreversible. Prior deep learning in spine CT, radiography and MRI has showed considerable potential, especially for the identification of lumbar spinal stenosis, deformity, and spinal osteoarthritis. Deep learning is still in its infancy when it comes to the identification and classification of spinal cord disorders on CT, radiography and MRI. It now focuses mostly on the detection, bone segmentation, and metastatic load [14-16]. Although, the existing segmentation and detection approaches for spinal cord disorder prediction fails to produce high detection rate and dice coefficient with erroneous labelling and localization of spinal cord components. Also, they failed to determine more than one spinal cord disorders at a time due to the processing of limited clinical data and unique characteristics related to diverse disorders are not extracted. Hence there is a need to propose a novel AI based point of care diagnosis model to effectively detect various spinal cord disorders by processing large clinical data images. The main contribution of this paper is as follows:

- In the labeling and segmentation of spinal cord images for the detection of spinal disorders, the erroneous label findings due to similar forms of vertebrae and missed vertebrae in segmentation is solved by using pipelined stochastic convolutional labelling NN and Multi-Atlas Instance SegNet in Pipelined labeling with level count Circular Localization.
- During the classification of spinal cord disorders based on their severity level Bilsky Phenotype grading classifier has been utilized to classify the diseases such as Spinal osteoarthritis, Lumbar Spinal Stenosis (LSS) and spinal deformities with their severity levels without centroid detection and it enhance the detection rate without misclassification.

Thus, the Pipelined Multilayer AI-based point-of-care model was created to effectively identify various spinal cord disorders with their sublevels at an early stage using accurate labeling, segmentation, and domineering feature extraction on the localized spinal cord components.The content of the paper is organized as follows: section 2describes related works, section 3 provides novel solution, the implementation results and its comparison are provided in section 4; finally, section 5 concludes the paper.

LITERATURE SURVEY

Al-kafri et al [17] described a method for semantic segmentation and delineation of lumbar spine MRI scans using deep learning to assist doctors in performing lumbar spinal stenosis detection. MRI scans from 515 patients with symptomatic back pain are included in this dataset. Expert radiologists make annotations on each study describing the lumbar spine's observed characteristics and state. Also, created a ground truth dataset with labels for four key lumbar spine areas, which wasutilised as training and test pictures for segmentation classification algorithms. Through a derivation of the Jaccard Index, two novel metrics, namely confidence and consistency, were devised to evaluate the caliber of the ground truth dataset. Using SegNet, tried out semantic segmentation. However, the mean accuracy in segmentation is consistently lower in the unregistered class.

Mushtaq et al [18] discusses the localization and segmentation of the lumbar spine, which aid in the analysis of lumbar spine abnormalities. YOLOv5, the fifth variation of the YOLO family, is used to locate the lumber spine. Then, linked the angles with the region size calculated from the YOLOv5 centroids to identify the lumbar lordosis and achieved a 74.5% accuracy. To acquire the segmented vertebrae and its edges, cropped images from YOLOv5 bounding boxes are sent through HED U-Net, a system that combines edge detection and segmentation. After employing a Harris corner detector with extremely minimal mean errors to find the corners of the vertebrae, the

lumbar lordortic angles (LLAs) and lumbosacral angles (LSAs) are discovered. Although, the complexity in location and segmentation process gets increased and there is a need to develop a fully automated machine learning toolkit for spinal deformities to prevent invasive surgery methods.

Chae et al [19] presented an automated method for precisely measuring spinopelvic parameters using a decentralized convolutional neural network in order to replace the current manual process, which not only necessitates skilled surgeons but also has processing limitations due to the explosion of big data technologies. The suggested approach involves gradually constricting the regions of interest (ROIs) for feature extraction, which causes the model to concentrate primarily on the crucial geometric properties represented as key points. Utilizing decentralized CNN involves distinct datasets, which must be given specifically for each order. As a result, it takes time to create the datasets as well as train the CNN models thoroughly. Although, the failure in detection arose because the L5 vertebra and sacrum's positions were incorrectly anticipated by the ROI detection stage of the second order ROI detection model.

Rehman et al [20] uses the probability map of a pre-trained deep network to initialize the level set and refines the output repeatedly under the operation of multiple factors. As a result, the network's learning ability is increased, and the network can accept large topological form changes in the vertebrae. On two separate datasets, the proposed technique was tested. The first is a collection of 20 publicly accessible 3D spine MRI datasets for disc segmentation, while the second is a set of 173 computed tomography scans for segmenting thoracolumbar (thoracic and lumbar) vertebrae. U-Net architecture, on the other hand, fails to perform and obtain suitable segmentation performance when dealing with segmentation situations with substantial topological shape variability.

Zhang et al [21] proposed a two-phase study with an exploration group of 120 Adolescent idiopathic scoliosis (AIS) and a validation cohort of 51 AIS with mean Cobb angles of 23° and 5.0° at the first visit each. In order to create a composite model for prediction, patients with AIS were tracked for a minimum of six years. Clinical parameters were gathered on the initial visit from standard clinical practice, and blood was tested for circulating markers. The composite model has a larger area under the curve than do the individual factors currently employed in clinical practice. The model had a sensitivity of 72.7% and a specificity of 90% after being validated by a separate cohort the initial study to propose and validate a prognostic composite model based on clinical and circulation characteristics that could objectively assess the likelihood that an AIS curve would proceed to a severe curvature. The study, however, did not provide information on the relationship between treatment outcome and disease severity.

In order to determine the extent of the damage and forecast the illness patterns on the excessively segmented regions and features, a novel segment-based classification model has been proposed by Ahammad et al [22]. The spinal cord areas in the current model are segmented using a hybrid image threshold technique in order to employ a non-linear SVM classification strategy. The suggested threshold-based non-linear SVM exhibits superior accuracy for spinal cord injury (SCI) detection than the conventional feature segmentation-based classification models. However, this model has to precisely maintain its performance in terms of accuracy and error rate. Additionally, the noises in the T1-weighted and T2-weighted regions are not optimized.

Glockeret al [23] proposed a robust localization and identification algorithm which builds upon supervised classification forests and avoids an explicit parametric model of appearance. Using the dense labels, to learn a discriminative centroid classifier based on local and contextual intensity features which is robust to typical characteristics of spinal pathologies and image artifacts. Quantitative evaluation is carried out with respect to localization errors and identification rates and compared to a recently proposed method. This approach is efficient and outperforms state-of-the-art on pathological cases. It will focus on improve the centroid estimation by employing intervertebral constraints.

Feulner et al[24] method for automatic localization and identification of vertebrae in arbitrary field-of-view CT scans. No assumptions are made about which section of the spine is visible or to which extent. The algorithm is based on regression forests and probabilistic graphical models. The discriminative, regression part aims at roughly detecting the visible part of the spine. Accurate localization and identification of individual vertebrae is achieved through a generative model capturing spinal shape and appearance. It will be increase the amount of training data, in particular, for the cervical region would produce an increase in accuracy across the entire spine.

Ahammadet al [25] presented a deep learning framework for helping diagnose SCI features based on the segmentation process. A real-time wearable sensor is used to capture the spinal cord disorder data with different shapes and orientations. Experimental results show that the present CNN-deep segmentation based boosting classifier has high computational SCI disorder prediction compared to the existing CNN based classifiers. This work can be extended to use deep learning framework with Hadoop approach.

Aarabi et al [26]is proposed traumatic spinal cord injury (TSCI) classification system using a convolutional neural network (CNN) technique with automatically learned features from electromyography (EMG) signals for a non-human primate (NHP) model. The proposed classifier is based on a CNN using filtered segmented EMG signals from the pre- and post-lesion periods as inputs, while the kNN is designed using four hand-crafted EMG features. The results suggest that the CNN provides a promising classification technique for TSCI, compared to conventional

machine learning classification. The performance of the two classifiers was measured and compared according to five performance metrics (accuracy, sensitivity, specificity, precision, and F-measure). It will help researchers learn about the effect of implement the CNN for such a TSCI data set.

From the analysis, it is noted that [17] the mean accuracy in segmentation is consistently lower in the unregistered class, [18] have high computational complexity, and [19] have error in detection. In [20], segmentation performance degrades with substantial topological shape variability, [21] provide very less information for clinical decision making, [22] have noise in the T1-weighted and T2-weighted regions, [23] improve the centroid estimation, [24] will be increase the amount of training data, in particular, for the cervical region, [25] extended to use deep learning framework with Hadoop approach and [26] implement the CNN for such a TSCI data set.

PIPELINED MULTILAYER AI BASED POINT OF CARE MODEL FOR DIAGNOSIS OF SPINAL CORD DISORDERS IN BIG CLINICAL DATA

The spinal cord disorder caused by Spinal osteoarthritis, Lumbar Spinal Stenosis (LSS) and spinal deformities arediminishes the quality of human life. This is determined by clinically scanned spine images, which are integrated AI algorithms into point of care (POCT) devices to diagnose a spinal cord disorder. The accurate diagnosis of spinal cord disorders requires the exact localization and segmentation of vertebrae. However, the existing labelling and localization method for scanned images of the spinal cord is unsuitable for large clinical data corroboration. Hence a novel, *Pipelined labeling with level count Circular Localization* method have been used to processed the large clinical data with spine CT scan images through the POCT, in which IIR - Hough Pipeline transform filtering improves image resolution and edge detection, making all vertebrae noticeable in the image. But the existing techniques have erroneous label results due to missed vertebrae that were only partly visible on the image, similar forms of vertebrae in the cervical, thoracic, and lumbar regions, and the labelling process failing to detect sacrum.Hencepipelined stochastic convolutional labelling NN fetch the similar form of the vertebrae and label individually as cervical/lumbar vertebrae and thoracic/sacrum vertebrae and maintain labeling without affect the detection of sacrum.During localization processprevious approaches localization error were hampered which occurs frequently in spinal cord images with anatomical abnormalities such as additional and transitional lumbar vertebrae, making it difficult to properly identify vertebrae in the mid-thoracic region.In which the additional and transitional lumbar vertebrae are determined using Level check counter NN and the vertebrae are correctly localised in all regions of the spinal cord component with its circular anisotropic localization mechanism, thereby eliminating localization error.

Furthermore during the segmentation of spinal cord regions, existing semantic and automated segmentation approaches require annotations in the form of bounding boxes and target region position, the intervertebral disc, sagittal region, and spinal canal are missed in segmentation results with low dice score. These localized spinal cord components are segmented using Multi-Atlas Instance SegNet, which provides smooth image details with a high dice score in segmenting the intervertebral disc, the sagittal region, and the spinal canal.Furthermore, existing models diagnose single spinal cord disorders using limited scanned images and do not extract significant angular, curvature, structural, and distance features, resulting in misclassification because the region-area-based method relies on the centroids of multiple vertebrae and even a small error in the centroids' computation affects the entire area.Hence a novel, *Domineering Feature Transformer based Classification* has been proposed to providethe effective diagnose of the spinal cord disorders at an early stage a novel, in which Visual bipartite matching loss feature transformeris used to discover cobb angle, area between anterior and posterior vertebra, end plate angle, local curvature, bone structure, and intervertebral distance and the different spinal cord disorders, such as lumbar spinal stenosis, spinal deformities, and spinal osteoarthritis, are classified with their sub-levels using the Bilsky Phenotype grading classifier without centroid detection, which improves the detection rate while avoiding misclassification.Overall, the proposed AI-based point-of-care model accurately diagnoses various spinal cord disorders and their sublevels at an early stage through accurate labeling, segmentation, and domineering feature extraction on localised spinal cord components.

Figure 1 depicts the proposed method's processing of large clinical data, in which IIR - Hough line transform filtering increases image resolution, allowing all vertebrae to be visible in the image, and then pipelined stochastic convolutional labelling NN labels all similar vertebrae separately. Thus, the cervical/lumbar vertebrae and thoracic/sacrum vertebrae are labeled, and labelling of various images were maintained with a single stage fetch of labels without failure in sacrum detection. The additional and transitional lumbar vertebrae are determined by the level check counter NN, and the vertebrae are then correctly localised in all areas of the spinal cord component using its circular anisotropic localization mechanism. Multi-Atlas Instance SegNet is used to divide these localised spinal cord components. The segmented components are processed through the neural network, and the features such as cobb angle, area between anterior and posterior vertebra, end plate angle, local curvature, bone structure, and intervertebral distance are extracted, and the various spinal cord disorders such as lumbar spinal stenosis, spinal deformities, and spinal osteoarthritis are classified with their sub-levels based on Bilsky Phenotype grading classification.

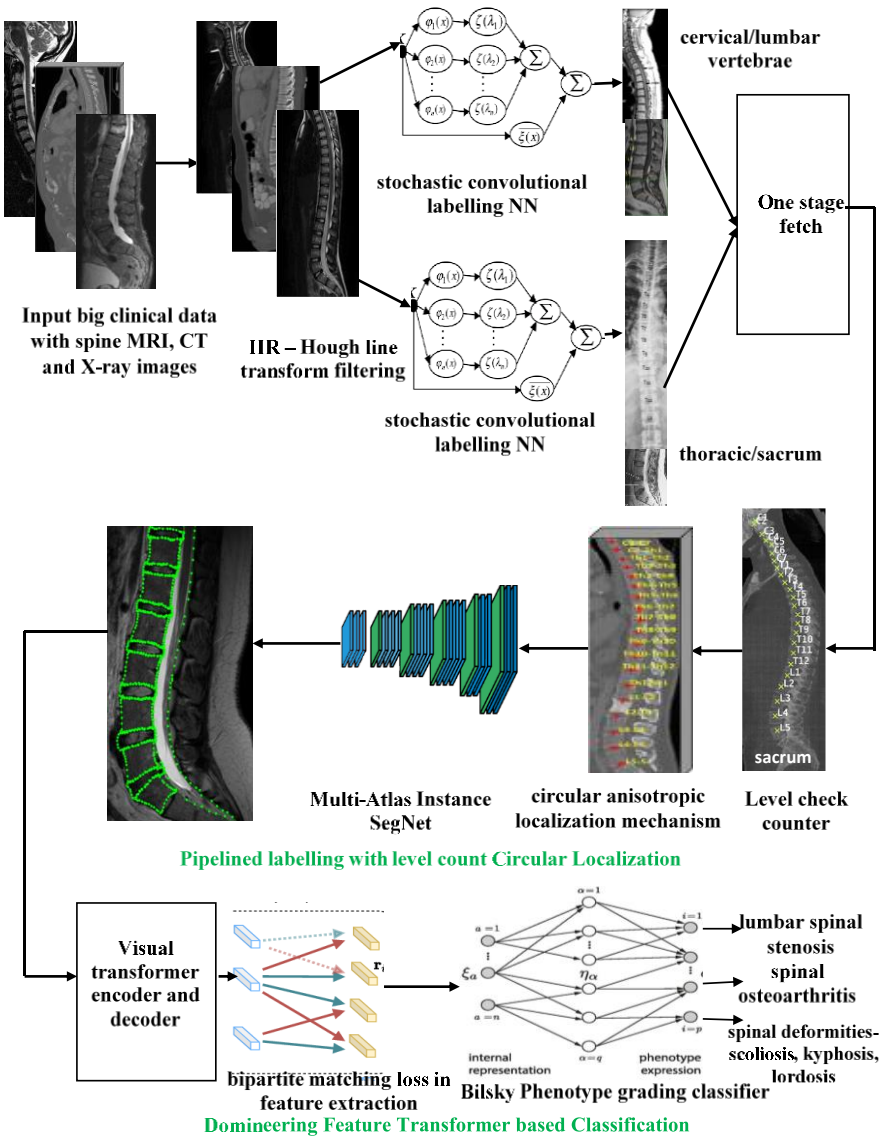

Figure 1: Architecture diagram of the Pipelined Multilayer AI based POCT model

Pipelined labeling with level count Circular Localization

Pipelined Labeling with level count Circular Localization has analyzed large amounts of clinical data from a large number of patients in order to provide an appropriate labelling and localization method for scanned images of the spinal cord. The accurate diagnosis of spinal cord disorders such as lumbar spine stenosis, spinal deformities, and spinal osteoarthritis requires the exact localization and segmentation of vertebrae. The POCT assists in determining the value of healthcare to patients, payers, providers, and vendors. Recently, the use of AI (artificial intelligence, machine learning, deep learning, expert systems, and neural networks) in diagnostics has grown.AI is easily incorporated into POCT devices in clinical pathology to provide result interpretation or diagnosis. To verify the efficiency of the AI algorithms, conventional laboratory testing results are used as a standard measure. POCT devices also play an important role in the prevention of infectious disease spread by providing real-time testing and lab-quality microbial diagnosis in minutes. Early detection and therapy optimization aid in the containment of infectious disease outbreaks. A slight decrease in the amount of back pain patients, associated medical care, or back pain intensity can have a substantial impact on socio economic costs, and many patients can benefit. The start and progression of spine diseases such as lumbar pain, herniated disk, spinal canal stenosis, and spondylolisthesis are all influenced by degenerative disc disease.

Large clinical data with spine CT scan images are processed using a novel in which IIR – Hough line transform filtering that increase the resolution of images with improved edge detection thereby all vertebrae are visible in image. IIR – Hough line transform filter is used to recover an image which is a property that applies to many linear time-invariant systems that have an impulse response h(t) that does not become precisely zero after a certain point,

$$a_0y(k) + \cdots . + a_{M-1}y(k - M + 1) = b_0x(k) + \cdots + b_{N-1}x(k - N + 1) \quad (1)$$

where at least one of the factors bi1iN1 is not zero. This is readily reduced to a relationship where $\boldsymbol{a_0}$ = 1. Equation (1) is verified for all the values of *k*.

$$y(k - 1) = -a_1y(k - 1) \ldots . -a_{M-1}y(k - M) + b_0x(k - 1) + \cdots . + b_{N-1}x(k - N) \quad (2)$$

Where y(k) depends on the previous values of the output y(k-2),..., y(k-M) and N + 1 values of the input signal x(k),..., x(k-N) by reinjecting equation (2) of y(k-1) in the difference equation in (1). Now express the output y(k) as a linear combination of an infinity of terms of the input signal x by repeating this process indefinitely (k). Thus the IIR filter is feasibly increase the resolution of the images and the filter images is detected by Hough transform.

Hough Line Transform has been modified to recognize other shapes such as circles and quadrilaterals of specific types. It is important to understand four concepts: edge image, the Hough Space, and the mapping of edge points onto the Hough Space, an alternate way to represent a line, and how lines are detected. An edge image is the output of an edge detection algorithm. An edge detection algorithm detects edges in an image by determining where the brightness/intensity of an image changes drastically. It is crucial to perform edge detection first to produce an edge image which will then used as input into the algorithm. This is used to determine whether a line exists in the edge image. An alternate way to represent a line is expressed in equation (3),

$$m = \frac{rise}{run} = \frac{y_2 - y_1}{x_2 - x_1} \quad (3)$$

Hough line transform mechanism used in used IIR – Hough line transform filtering detect straight lines in images, which is maps the edge points in an image onto the polar coordinate system. Then, to extract all vertebraes edges area and use the Hough Lines transform algorithm to extract the optimal spinal veritebrae edges.

Algorithm 1. Hough Line Transformation Mechanism in INR-Hough Line Transform Filter

Step 1. Decide on the range of ρ and θ. Often, the range of θ is [0, 180] degrees and *ρ* is [-*d*, *d*] where *d* is the length of the edge image's diagonal. It is important to quantize the range of ρ and θ meaning there should be a finite number of possible values.

Step 2. Create a 2D array called the accumulator representing the Hough Space with dimension (*num_rhos*, *num_thetas*) and initialize all its values to zero.

Step 3. Perform edge detection on the original image. This can be done with any edge detection algorithm of your choice.

Step 4. For every pixel on the edge image, check whether the pixel is an edge pixel. If it is an edge pixel, loop through all possible values of θ, calculate the corresponding ρ, find the θ and ρ index in the accumulator, and increment the accumulator base on those index pairs.

Step 5. Loop through all the values in the accumulator. If the value is larger than a certain threshold, get the ρ and θ index, get the value of ρ and θ from the index pair which can then be converted back to the form of $y = ax + b$.

Thus, the Hough Transform algorithm detects lines by finding the (ρ, θ) pairs that have a number of intersections larger than a certain threshold. Thus IIR-Hough line transform filtering increase the resolution of images with improved edge detection thereby all vertebrae are visible in image. After the image detection all spinal vertebraes are label by Pipelined stochastic convolutional labelling NN such as cervical/lumbar vertebrae and thoracic/sacrum vertebrae separately.

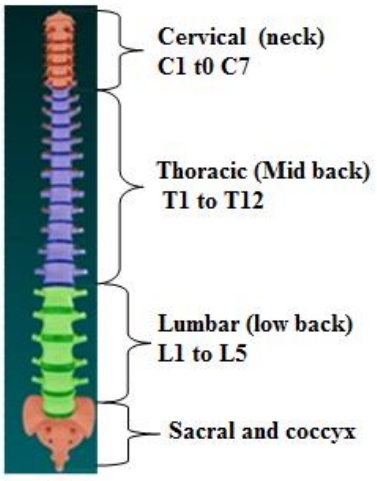

Figure 2: Structure of spinal cord

Figure 2, shows the pipelined stochastic convolutional labelling NN will be used to label all visible vertebrae pictures. It is queried for spine labels depicting the cervical/lumbar vertebrae and thoracic/sacrum vertebrae

separately. In total, 475 lumbar and 245 cervical cases were retained, containing 465/438 and 223/221 T1−/T2-weighted image series, and 3456 and 2321 spine labels, respectively. Both T1- and T2-weighted images and that the number of labeled vertebrae per case varied, although all vertebraes label as L1-L5, C2-C7, T1-T12 and S1 for the cervical/lumbar vertebrae and thoracic/sacrum vertebrae respectively. Since the pipelined stochastic convolutional labelling NN for spine labeling involves placing spine labels in the single image.

Pipelined stochastic convolutional labelling NN have two stochastic CNN that used a network design that included two convolutional (C) layers followed by a max-pooling (MP) layer, two more C layers followed by an MP layer, and two fully connected (FC) layers before the output layer. Except for the output layer, which used a soft-max function, all levels used a leaky rectify function as an activation function. The C and MP levels each had three receptive fields. The size of the image patches and field-of-view varied slightly between CNNs, owing mainly to the estimated size of the relevant vertebrae. The patch sizes for the lumbar and S1 CNNs were 24×24 and 32×32 respectively, with a spatial precision of $2 \times 2mm^2$. The patch area of the cervical and C2 CNNs was 32×32 with a spatial resolution of $1 \times 1mm^2$. The proposed model labels them to provide a detection and label configuration that most closely matches previously seen spine label configurations based on label order and spatial locations.

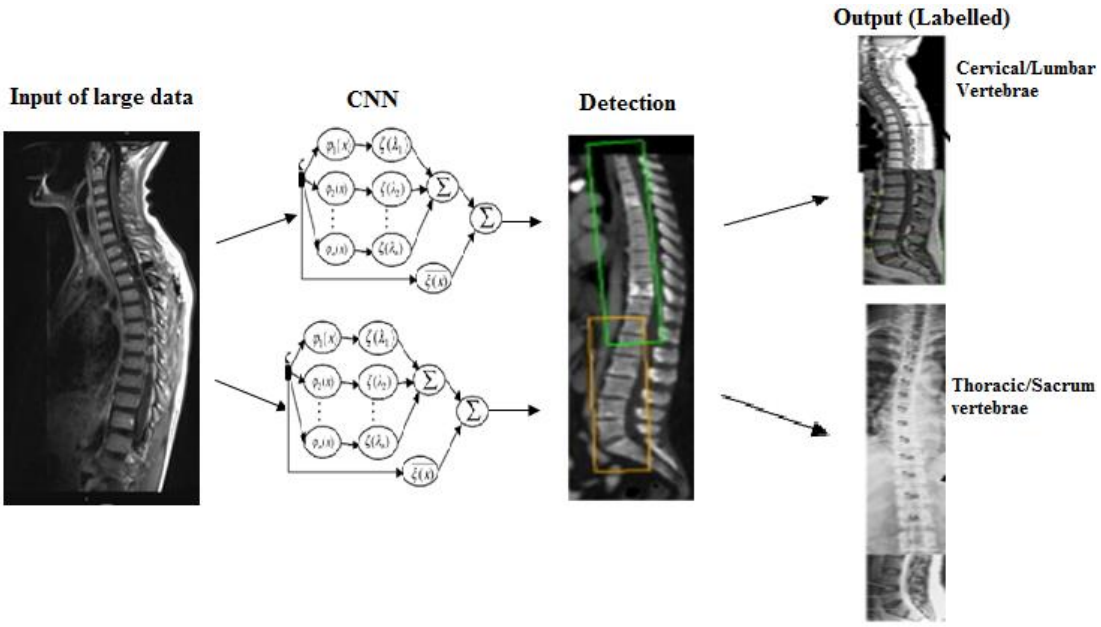

Figure 3: Spinal vertebrae labeling by pipelined CNN

Figure 3 depicts the labelling process for spinal vertebrae. Image patches are extracted from the original image and fed into pipelined CNNs, which provide positive pixel-by-pixel detections for image patches that match to a vertebra. The centroids of the detections are kept after connected component analysis of the detection maps and fed to a parts-based graphical model, which discards false positive detections and labels the remaining detections. This produces a collection of annotated spine labels as the end result. All affirmative detections from each CNN were grouped using connected component analysis, with the centroid and area of each connected component returned as detection step output. As a result, for each vertebra detection i, a location $x_i$and chance $p_i$are provided.A layered (one layer for each expected vertebrae to label) graph *G = (V, E)* with vertices $v_{i,l} \in V$ for every vertebra detection, $i \in (1, ..., N)$ and expected vertebrae to label, $l \in (1, ..., L)$ was constructed, with the layers in a stack according to the anatomical order of the vertebrae labels and only allowing edges between adjacent layers. The distance function of each edge $\delta(v_{i,l}, v_{j,l+1})$ was defined an equation (4).

$$d\,l\,(x\,i, x\,j\,) = (y\,i, j - \mu\,l\,)\,T\,\Sigma - 1\,(y\,i, j - \mu\,l\,) \times 1/(p\,i \times p\,j\,) \quad (4)$$

where y(i,j)= x j − x i. The variables l, l, and R l are inferred from the training data and correlate to the mean displacements (1,..., L1), covariance matrices of displacements (1,..., L1), and allowed ranges for displacements (R 1,..., R L1) between each set of adjacent vertebrae. Hence, finding the shortest path while including as many labels as possible, will provide the optimal configuration of vertebrae as given by all vertebra detections. The pixels of each picture were coarsely divided into four groups based on the provided spine label locations: vertebra centre regions, intervertebral disc regions, vertebral edge regions, and background. Given that the spine labels only correlate to a single point for each vertebra, there was a need to increase the number of image patches that could be used for training.

For training and validation, all image patches matching to vertebral center regions were kept as positive examples, whereas image patches from the other regions were randomly chosen to have the same number of samples as the positive samples from each of the three categories. As a result, the data contained roughly equal amounts of samples from each of the four groups. Furthermore, the suggested method, pipelined stochastic convolutional labelling NN, labels all similar forms of spinal vertebrae in the cervical, thoracic, and lumbar regions. In one step, the next images are fetched from the memory address presently stored in the programme counter and stored in the instruction register. The PC refers to the next instruction that will be read at the next cycle at the conclusion of the fetch operation. As a result, it is possible to keep labelling various images without failing sacrum detection. However, all labeled spinal vertbraeshas to be labeled and localized properly by determining theadditional and transitional lumbar vertebrae.

Thus the Level check counter NN method is proposed to determined anatomical abnormalities due to the additional and transitional lumbar vertebraes. Lumbosacral transitional vertebra (LSTV) is a congenital spine anomaly caused by Hox gene mutations that cause sacralization (fifth lumbar vertebra shows assimilation to the sacrum) and lumbarization (first sacral vertebra shows lumbar configuration), as determined by Level check counter NN. This has an impact on either L5 or S1. Unfortunately, imaging classification systems for LSTVs do not provide insight into accurate vertebral labelling information. The training database and goal pairs of input are required for supervised training of the NN. The primary goal is to reduce the differentiation between target pairs, which is accomplished by optimizing network weights. The Level check counter NN is made up of three layers: output, input, and the recurrent concealed layer. The layer's input is a sequence of vectors at the time an equation is expressed. (5).

$$H_\tau = H_1, H_2, \ldots., H_6 \quad (5)$$

The inputs in the fully connected check counter NN are given to the hidden units in which the connections are represented by the weight matrix. The hidden layer consists of i hidden units that are joined to each other through recurrent connections and the time and is given an equation (6).

$$Z_r = F_1, F_2, \ldots., F_i \quad (6)$$

The hidden layer represents the memory or state space of the system, given in equation (7).

$$Z_r = W_r(A_r) \quad (7)$$

$W_r(A_r)$indicates the hidden layer activation function, and A denotes the output gate. The portion of memory content that is exposed is determined by spinal cord level detection. The output gate is written an equation (8).

$$Z_r = W_r(A_r = \omega_{lk} H_z + \omega_{kk} F_{\tau-1} + a_{hidden} \quad (8)$$

where ahidden represents the bias of hidden units and the term signifies the weight matrix. The hidden units that are connected to the hidden layer are denoted by the symbol kk. Equations (7) and (8) show that the level by NN is made up of nonlinear state equations that are iterated over time. With the help of an input vector, the concealed layer predicts at the output layer for each time step. The hidden state NN is the set of values that summarizes all unique information about the past states of the network over several time steps. This combined information to identify the future behavior of the network to make accurate predictions in the output layer. Thus additional and transitional lumbar vertebrae are detected using level check counter NN. Then circular anisotropic localization mechanism identifies the location of the spinal vertebrae in an image and draws a bounding box around the vertebraes.The annotated spine dataset is passed through YOLOv5 to obtain the localize vertebrae. Bounding boxes across each vertebra are used to crop the images. For the localization of the spine bone, circular anisotropic localization technique was utilized after that Multi-Atlas Instance SegNet method was implemented for vertebral body segmentation.

A three-dimensional anisotropic diffusion filter is applied to the bias-field corrected image for image smoothing while preserving edges. Consider xk $\in R^2$as a random variable that assigns a scored spinal vertebrae sk to its image location. Let pk(xk, I) be a function that gives the score value of a pixel at location xk in the image I for the vertebraesk where 1 ≤ k ≤ 11. x = {x1, x2 . . . , x11} denotes a configuration of spinal cord vertebrae. The optimal configuration x 0 = {x1, x2 . . . , x11} assigns the centers of all vertebrae s = {s1, s2 . . . , s11} to their exact locations. It find the optimal configuration x=0 with the maximum a posteriori (MAP) estimate in equation (9).

$$x' = argmaxP(x|I, \alpha) \quad (9)$$

where α represents the geometrical parameters learned from the training set and I is the image.$P(x|I, \alpha)$captures the local information about being a lumbar vertebrae and its relation with the neighboring vertebrae. The potential function $E_{Local}(x_k, I)$ is for the local information about the target structures for which isdirectly use the score values generated by fitting a logistic model to outputs of SVM is given equation (10).

$$E_{local}(x_k, 1) = -P_k(x_k, J) \quad (10)$$

For localization of individual vertebrae centroids, todefine a centroid density estimator an equation (11).

$$d_v(x) = \sum_{i=1}^{N} P(v) f(x_i)) \exp\left(\frac{||x - x_i||^2}{h_v}\right) \quad (11)$$

where {xi} N i=1 are image points for which p(v|f(xi)) > 0. Thus the vertebrae are localized properly in all areas of spinal cord component with its circular anisotropic localization mechanism thereby eliminate localization error.

These localized spinal cord components are segmented using Multi-Atlas Instance SegNet that provide smooth image details with high dice score in segmenting intervertebral disc, sagittal region, and spinal canal.Multi-atlas segmentation has become the standard segmentation framework due to its ability to quickly and accurately generalise structural information from labelled examples which is a special form of image segmentation that deals with detecting instances of vertebrae and demarcating their boundaries. It finds large-scale applicability in real-world scenarios. The multi-atlas instance segmentation method is divided into three separate stages: selection of the most similar subset of the database, pairwise deformable registration and finally label fusion. Thus, defining Ls as the label on atlas s amongst the S selected subjects on equation (12).

$$L(x) = round\ (\frac{\sum s=1,\ldots,sL_S(x)}{S}) \quad (12)$$

Let F_T represent the target image to be segmented and $A_1 = (F_1, S_1), \ldots., A_n = (F_n, S_n)$ represent the n atlases.$F_i\ and\ S_i$represent the ith warped atlas image and its corresponding warped manual segmentation obtained by performing deformable image registration to the target image. For the target image, each atlas generates one candidate segmentation. Some segmentation errors may exist in each of the candidate segmentations. Label fusion is the process of integrating the candidate segmentations produced by all atlases to improve the segmentation accuracy in the final solution. Thus to provide a final segmentation in equation (13)

$$S_T(x) = argmax_{l\in\{1\ldots.L\}} \sum_{i=1}^{n} S_i^l(x) \quad (13)$$

where *l* indexes through labels and *L* is the number of all possible labels, *x* indexes through image pixels. $S_i^l(x)$ is the vote for label *l* produced by the i_{th} atlas, defined by:

$$S_i^l(x) = \begin{cases} 1 & if\ S_i(x) = l \\ 0 & otherwise \end{cases} \quad (14)$$

Assume that atlas Ai gives correct labels with probability pi for the target image. The probability that the atlas will generate any specific wrong label can be roughly estimated by (1−pi)/(L−1). When pi > (1−pi)/(L−1), the atlas works better than random guess. When segmentation errors produced by different atlases are independent, the likelihood of multiple atlases agreeing on the same incorrect label is exponentially suppressed compared to the likelihood of them agreeing on the same correct label. Hence, the combined results are expected to produce significantly fewer errors than those produced by any single atlas and instance segmentation network to segment the specific vertebrae in CT images. First, an initialization locator module was set up to provide an initial locating box. Then the dual-output network was designed to segment two adjacent vertebrae inside the locating box. Finally, iteration was performed until all the expected vertebrae were segmented. Instance Segmentation is a special form of image segmentation that deals with detecting instances of objects and demarcating their boundaries. This procedure uses either a top-down or bottom-up approach, which means that the vertebrae are segmented sequentially from top to bottom, or vice versa. Even if numerous unsegmented vertebrae are visible, the network segments the first following not yet segmented vertebra. Other vertebrae that are the second or third not yet segmented vertebra in the traversal direction are ignored until they become the first not yet segmented vertebra in a later run. As a result, each network instance has a fixed traversal path. When a vertebra is in the centre of the patch, the patch size is selected to always include a portion of the next vertebra. This analyses a single patch iteratively centred at xt, where t indicates the iteration step. Initially, the patch is moved across the image in a sliding window manner with constant step size x, looking for the top-most vertebra in a top-down approach or the bottom-most vertebra in a bottom-up approach. The patch is moved towards a big enough fragment of vertebral bone as soon as the network detects it. The centre of the discovered fragment's bounding box, denoted as bt, becomes the centre of the next patch is represented in equation (15).

$$x_{t+1} = \begin{cases} x_t + \Delta x, if\ v_t < v_{min} \\ [b_t] \quad ,otherwise \end{cases} \quad (15)$$

When the position has converged, the segmented vertebra is added to the output mask with the help of a unique instance label and the segmentation mask acquired at this final position. In addition, the instance memory is refreshed. The network analyses the same patch again in the next version. The network is prompted by the updated memory to identify a fragment of the next vertebra, and the patch is moved to the centre of the detected new fragment, repeating the segmentation process for the next vertebra. If no fragment of the next vertebra is visible, traversal reverts to a sliding window motion until the next vertebra is discovered. The procedure is repeated until no more fragments are discovered, i.e., until all visible vertebrae have been segmented. For each vertebrae, the overall loss function of the multi-atlas instance segmentation is calculated using Equation (16).

$$L = L_{detection} + L_{instance\ segmentation} \quad (16)$$

Where$L_{detection}$ loss function is given according to Equation (17).

$$L(P_i, t_i) = \frac{1}{N}\sum_{i=1} |P_i^* - P_i|^2 + \alpha \frac{1}{N}\sum_i P^* L_{loc}(t_i, t_i^*) \quad (17)$$

whereP_i is the predicted probability of vertebrae i, is the ground truth of vertebrae i, t_i stands for the coordinates predicted, is the coordinates ground truth, N is the normalization term and α = a is the balancing parameter. The Linstance segmentation loss function is identified using the per-pixel sigmoid and average binary crossentropy to generate boundaries for each class, as shown in Equation (18)

$$L_{instance\ segmentation} = -\frac{1}{S^2}\sum_{1\le i,j\le s}\left[y_{ij} log y_{ij}^{k} + 1 - y_{ij} \log\left(1 - y_{ij}^{k}\right)\right] \quad (18)$$

where is the ground truth of boundaries of size region (S^2),y_{ij}^{k} is the predicted value of boundaries and k is the ground truth class.

Algorithm 2. Multi-Atlas InstanceSegmentation

for each control point z do
pre-select M atlas patches
for atlas patch I do
evaluate the augmented features fi
end
train the SVMz at z using {(fi, li)|i = 1, 2, ⋯ , M}
end
for each voxel x do
evaluate the augmented features fx
for each control point z near x do
determine the label lx,z to fx
end
if mode == 'training': then
ground-truth-values = values from the training dataset bbox,
classes = classifier(rois)
target-detection = Detection-Target-Layer(ground-truth-values) instance
segmention = instance-segmention (roisfromtarget detection)
loss = loss-functions(target-detection, bbox, classes, instance-segmention) algorithm
= [bbox, classes, instance-segmention,loss]
else
bbox, classes = classifier(rois)
target-detection = Detection-Layer(bbox, classes)
instance-segmention = instance-segmention (rois)
algorithm = [bbox, classes, instance-segmention]
end
determine the label lx by combining lx,z
end

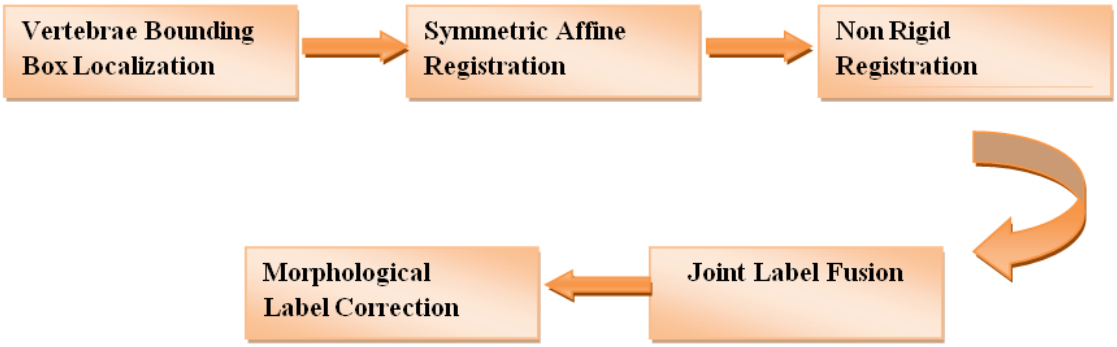

Figure 4: Multi-Atlas Instance for spine segmentation

Thus proposed a multi-atlas joint label fusion framework for spine segmentation on a vertebral basis is shown in figure 4. The automatic generation of a bounding box for each vertebra offered better local anatomical coherence between images and enabled for more precise image registration. To capture the geometric variability of vertebrae, an intensity-based non-rigid B-spline registration method with affine initialization was used. Following registration, the computed transformations were used to deform a collection of segmented atlases to the target space. The Dice coefficient (DC) used to assess segmentation precision. They are described in equation (15)

$$DC = \frac{2*|GT \cap S|}{|GT|+|S|} * 100\% \quad (15)$$

where GT and S which refer to the ground truth and the computed segmentations respectively. All transformed atlases were then combined using a joint label fusion method that determined the label based on local appearance similarity between each registration result.Finally, morphological label correction was used to correct over-segmented results that could not be correctly localised to a single vertebra. This step was used to correct under-segmented findings caused by the osteoporotic test cohort's relatively low spinal bone density. Thus, the localised

spinal cord components are divided using Multi-Atlas Instance SegNet, which provides smooth image details with a high dice score when segmenting the intervertebral disc, sagittal region, and spinal canal.

Domineering Feature Transformer based Classification

Domineering Feature Transformer based Classification is proposed to effectively diagnose spinal cord disorders at an early stage, in which cobb angle, area between anterior and posterior vertebra, end plate angle, local curvature, bone structure, and intervertebral distance are extracted using Visual bipartite matching loss feature transformer.

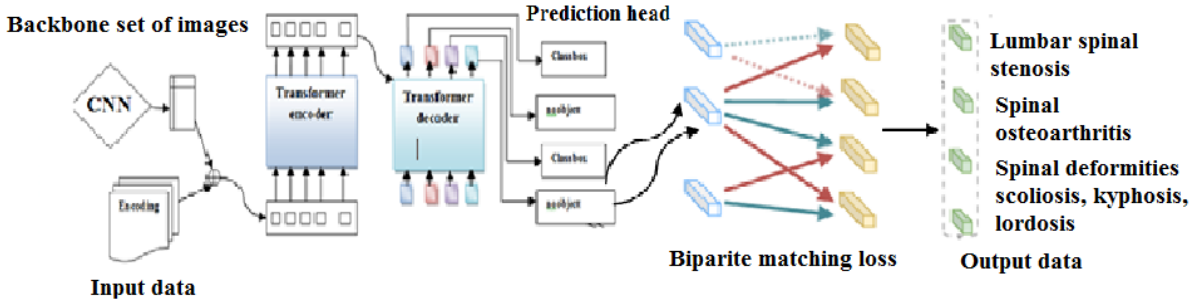

Figure 5: Visual bipartite matching loss feature transformer

Figure 5 shows a CNN backbone to derive a compact future representation, an encoder-decoder transformer, and a prediction head are the three major components. Following feature extraction by CNN, 1x1 convolution will decrease the channel dimension of CNN's final outputs. Because the transformer is permutation invariant, the set positional encoding comes before the input transformer encoder. The transformer encoder differs from the originals. Instead of decoding one image at a time, it decodes N outputs in parallel for N inputs. The ultimate forecasts will be computed. Finally, it forecasts the centre coordinates (normalized), height and width, cobb angle, anterior-posterior vertebral area, end plate angle, local curvature, bone structure, and intervertebral distance. DETR employs bipartite matching, or one-vs-one matching, by matching numerous bounding boxes to a single ground truth box. It is able to greatly reduce low-quality predictions and eliminate output reductions by conducting one-to-one matching. Loss in DETR is calculated by the sum of bipartite matching loss is given (16)

$$\dot{\sigma} = argmin \sum_i^N L_{match}(y_i, y_\sigma(i)) \quad (16)$$

Bipartite matching loss feature transformeris processed to extract the features of large clinical data such cobb angle, area between anterior and posterior vertebra, end plate angle, local curvature, bone structure and intervertebrae. This approach is 'order' agnostic. Optimal matching is calculated using the Hungarian algorithm is given in equation (17)

$$L_{Hungarian}(y, \hat{y}) = \sum_{i=1}^N \left[-log P_\sigma(\iota)(c_\iota) + 1_{\widehat{\{c_\iota \neq 0\}}} L_{box}(b_\iota, \widehat{b_\sigma(\iota)}) \right] \quad (17)$$

This loss calculation takes both class and boxes into consideration. The process of matching is similar to heuristic processes used in previous work where match region proposals or anchors to the ground truth object. Thus, the Visual bipartite matching loss feature transformer is used to derive cobb angle, area between anterior and posterior vertebra, end plate angle, local curvature, bone structure, and intervertebral distance. The grading scale is important for treatment planning and consists of a six-point classification, which can be subdivided into two key groups. Low-grade disease (0, 1a, and 1b grades) can be targeted for initial radiotherapy (e.g., external beam radiotherapy or stereotactic radiosurgery) and high-grade disease (1c, 2, and 3 grades) with contact or compression of the spinal cord can be considered for initial surgical decompression and subsequent radiotherapy.

The Bilsky Phenotype grading classifier, also known as the Bilsky scale, is used to determine how much vertebral body spread has compromised the spinal canal and whether cord compression exists. It could be used to determine when action (radiotherapy or surgery) is necessary. The system uses axial T2-weighted images at the site of most severe spinal canal compromise. The scale is nominally a 4-point scale, but grade 1 is further subdivided into 1a, 1b and 1c, making it a 6-point scale in practice. Increasing grades denote increasing degrees of stenosis.

- **grade 0**: bone-only disease.
- **grade 1**: epidural extension without cord compression.
  - **1a**: epidural extension only (no deformation of the thecal sac).
  - **1b**: deformation of thecal sac, without spinal cord abutment.
  - **1c**: deformation of the thecal sac, with spinal cord abutment.
- **grade 2**: spinal cord compression, with cerebrospinal fluid (CSF) visible around the cord.
- **grade 3**: spinal cord compression, no CSF visible around the cord.

In the absence of mechanical instability, grades 0, 1a, and 1b are considered for radiation as initial treatment, the role of surgery and radiosurgery in patients with grade 1c epidural is controversial with high-dose hypo fractionated radiation as a possible SRS option2. Grades 2 and 3 describe high-grade epidural spinal cord compression and,

unless the tumor is highly radiosensitive, require surgical decompression prior to radiation therapy. As a result, the suggested model for grading metastatic epidural spinal cord compression on staging CT scans was developed. When compared to general and specialised radiologists, the Bilsky Phenotype grading classifierhad better interobserver agreement for the detection of trichotomous Bilsky grading (normal, low, and high-grade). When there is no indication of high-grade disease on CT, this model is used to triage patients for minimise the need for anCT scan images. The different spinal cord disorders, such as lumbar spinal stenosis, spinal deformities, and spinal osteoarthritis, are classified with their sub-levels using the Bilsky Phenotype grading classifier without centroid detection, which improves the detection rate while avoiding misclassification.

Overall the proposed model to produce high detection rate and dice coefficient with labelling and localization of spinal cord components. Also, they to determine more than one spinal cord disorders at a time due to the processing of large clinical data. Hence the proposed novel AI based point of care diagnosis model effectively detect various spinal cord disorders by processing large clinical data images.

RESULT AND DISCUSSION

This section describes about the implementation outcomes, the performance of the proposed system, and a comparison section to make sure the proposed system is appropriate for effectively detect various spinal cord disorders by processing large clinical data images.

System configuration

This section provides a detailed description of the implementation results and the performance of the proposed system to ensure that the proposed technique performs better and diagnosis the various diseases of spinal cord disorder.

This work has been implemented in the working platform of Python with the following system specification and the simulation results are discussed below.

OS : Windows 10
software : Python
RAM : 8 GB RAM
Processor : Intel i3

Data set description

The Spine database consists of spine-focused (i.e. tightly cropped) CT scans of 125 patients with varying types of pathologies. For most patients, multiple scans from longitudinal examinations are available, resulting in overall 242 scans in the database. For each scan, manual annotations of vertebrae centroids are provided. The data has been acquired at the Department of Radiology at the University of Washington [23], [24].

Simulated output of proposed model

The Simulated Output of the proposed model for diagnosis the various spinal cord disorderby processing large clinical data images has been explained in this section from the initial setup.

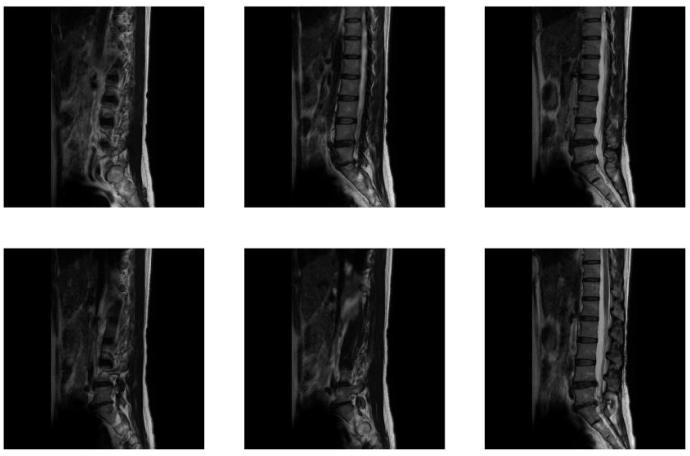

Figure 6: Input Large CT scan images.

Figure 6, shows the large input clinical data based on the CT scan for diagnosis the various spinal cord disorder. Diagnosis of spinal cord disorders such as spinal oncology, spine osteoarthritis, trauma, infections, degenerative diseases, and adult spinal deformity. The most common causes of back discomfort are spinal osteoarthritis, Lumbar Spinal Stenosis (LSS), and spinal deformities. Hence AI can be easily integrated into POCT in clinical pathology to keep the quality of big clinical data and generate effective findings when interpreting diseases using automated diagnostic classifiers.

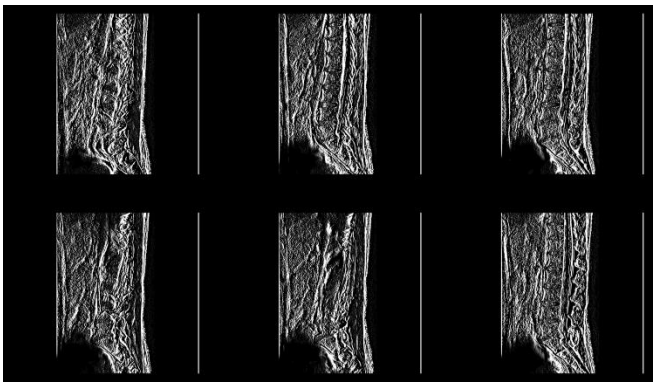

Figure 7: Filtered image

Figure 7 shows the filter image from the input of large number of scanned image. The proposed method to suggest the IIR filter that the output images from the filter is computed by using the current and previous inputs and previous outputs images. Because the filter uses previous values of the output, there is feedback of the output in the filter structure. Thus the filter to increase the resolution of all images.

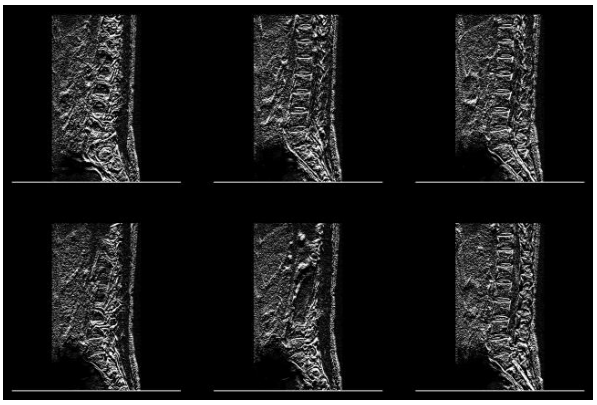

Figure 8: Edge detection of the input images

Figure 8, shows the edge detection of the resolution image from the large scanned images. In Hough line transform techniques to increase the edge detection. The result of an edge detection algorithm is an edge image. An edge detection algorithm finds edges in images by determining where the brightness/intensity of an image drastically changes.It is critical to conduct edge detection first in order to generate an edge image that will be used as input into the algorithm. Thereby all vertebraes are visible in the output image.

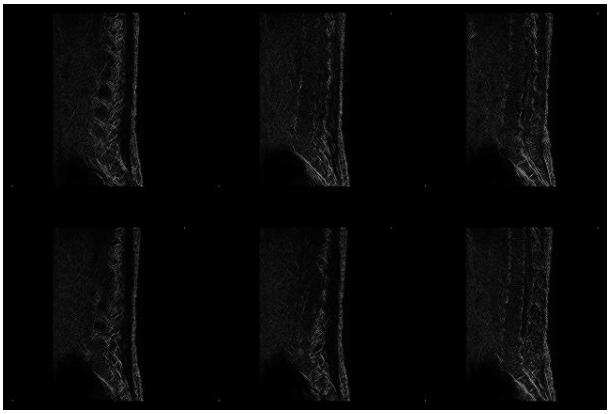

Figure 9: Labeling thefiltered CT scan images.

Figure 9, shows the labelling images. Where stochastic convolutional labellingNNislabeling the similar forms of vertebrae the overall images. Where cervical/lumbar vertebrae and thoracic/sacrum vertebrae are separately labeled in which one stage fetch of labels feasibly maintain labelling of different images without failure in sacrum detection. Moreover it determine the the additional and transitional lumbar vertebrae.

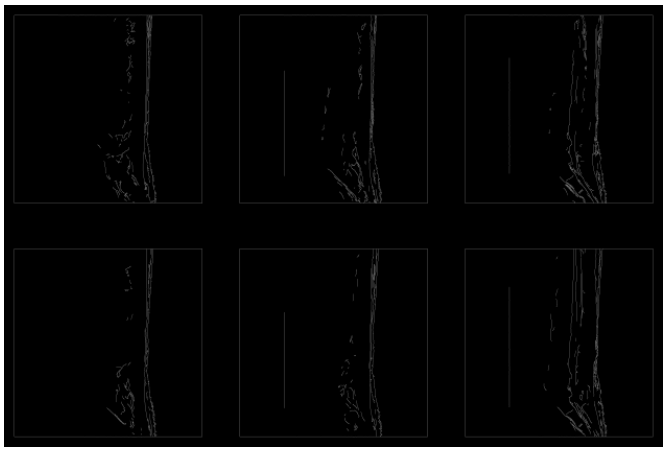

Figure 10: localization of spinal cord

Figure 10, show the localized images. Whichare localized properly in all areas of spinal cord component with its circular anisotropic localization mechanism. In regression label construction offers an adaptive configuration for predicting each vertebra. It is a supervised learning method for the probabilistic estimation of continuous variables that has shown excellent performance in the localization of anatomical vertebrae in CT scans using the circular anisotropic localization mechanism.

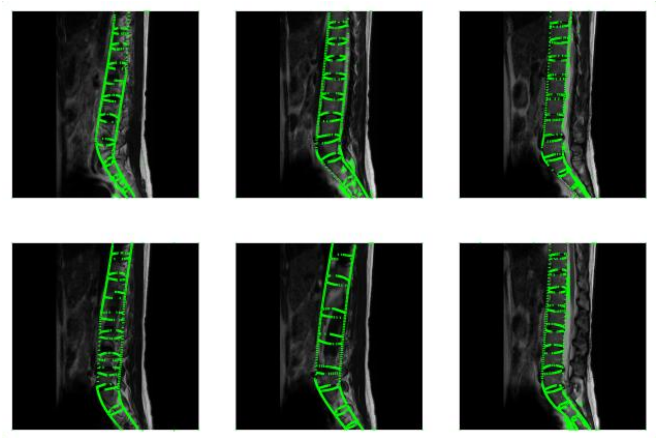

Figure 11: Segmented the spinal cord.

Figure 11, shows that were the spinal cord are segmented. Multi-Atlas Instance Segmentation techniquesto segment the each vertebraes. Segmentation of the vertebrae refers to the embryonic developmental process that results in the formation of the spine with a series of divided, similar anatomical units, that are the vertebrae. A key part of this process is somitogenesis. Thereby the proposed method provide smooth image details with high dice score in segmenting intervertebral disc, sagittal region, and spinal canal.

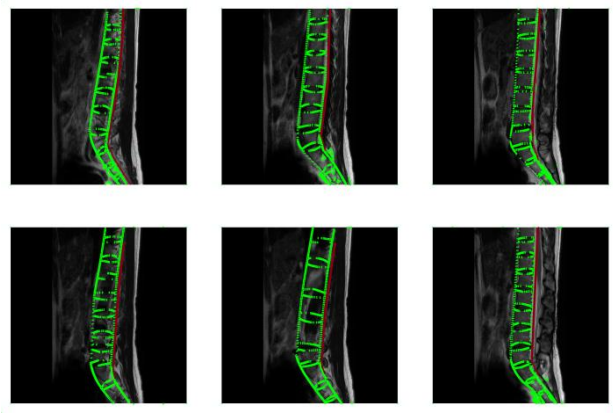

Figure 12: Binary segmenting intervertebral disc

Figure 12, shows that intervertebral disc are segmented, which is represent by red colour in the figure. Where the high dice score in spinal cord vertebrae is segmented. The image on the extreme left shows an anterior-posterior subluxation of the vertebrae. The image in the middle shows gaps on the vertebral boundary, which may be physiological due to vessel injection at this segmentation. A number of vertebrae are segmented together as a single spine object.

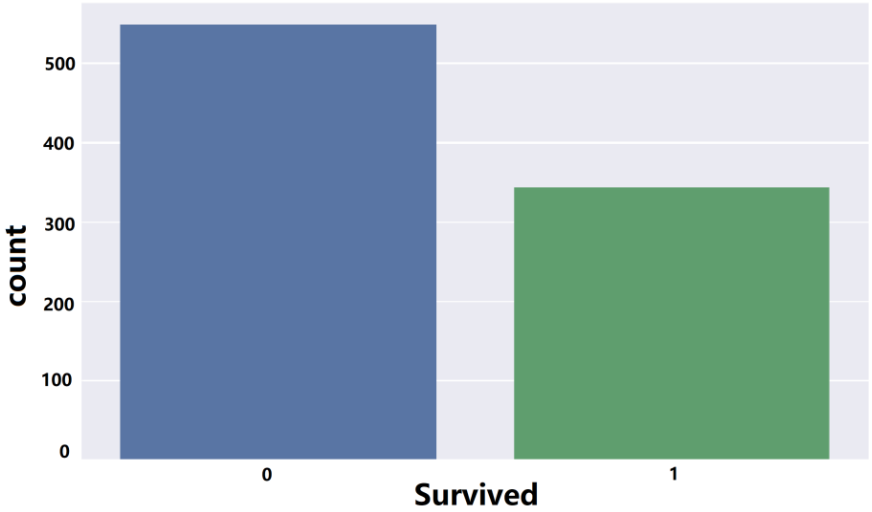

Figure 13: Severity count based on survived count of the proposed system

Figure 13, shows the survived count, which is compared with total number of spine dataset of the proposed system. Initially 500 numbers of data in the spine data set. The proposed method has to survive at the count of 300 which reduce the survived count based on the data set. Thus the proposed methodology has effectively diagnose various spinal cord disorders at an early stage with accurate labelling, segmentation and domineering feature extraction on the localized spinal cord components.

Performance metrics of the proposed system

In this section, a detailed explanation of the effectiveness of the suggested technique and the result is provided.

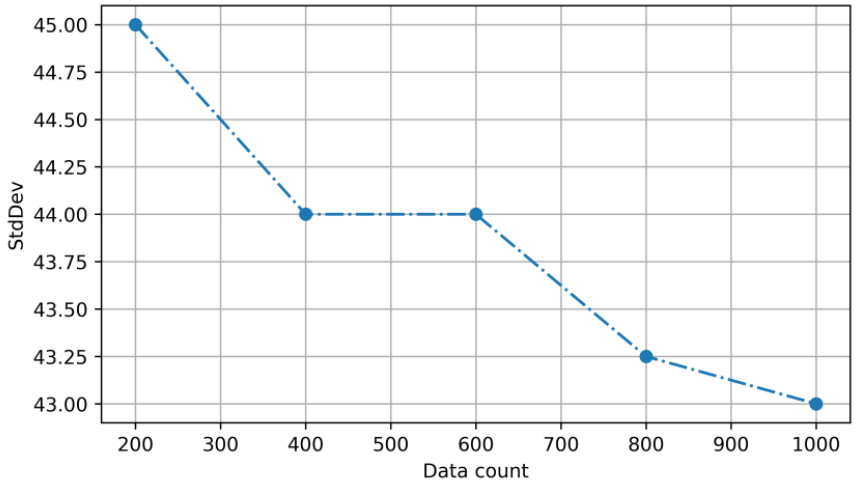

Figure 14: Standard deviation of the proposed system

The standard deviation of the proposed system for varying the number of input has been shown in figure 15. The standard deviation of the proposed system achieves a minimum value of 43.00 when the number of samples is increased and attains a maximum value of 45.00 when the number of images is reduced. The standard deviation of the proposed system has been decreased by using pipelined stochastic convolutional labelling NN that eliminate all the error during the labeling process.

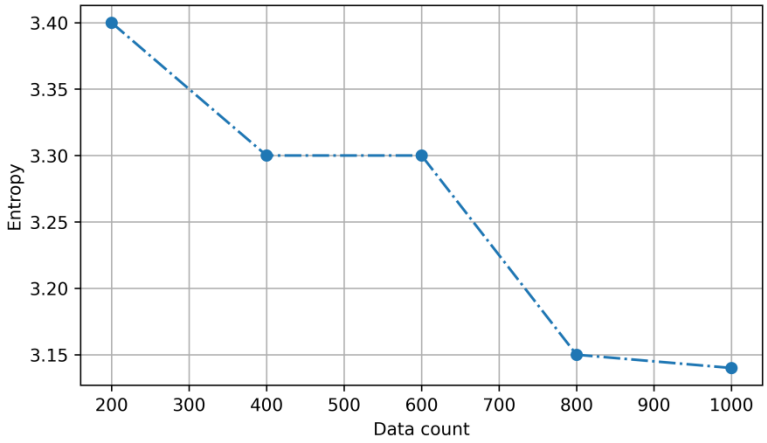

Figure 15: Entropy of the proposed system.

The entropy of the proposed system for varying the number of input has been shown in figure 15. The Entropyof the proposed system reducing the value of 3.12 when the number of samples is increased and attains a maximum value of 3.40 when the number of images is reduced. The entropyof the proposed system has been decreased by using level check counter CNN that determine the additional and transitional lumbar vertebrae of the spinal cord.

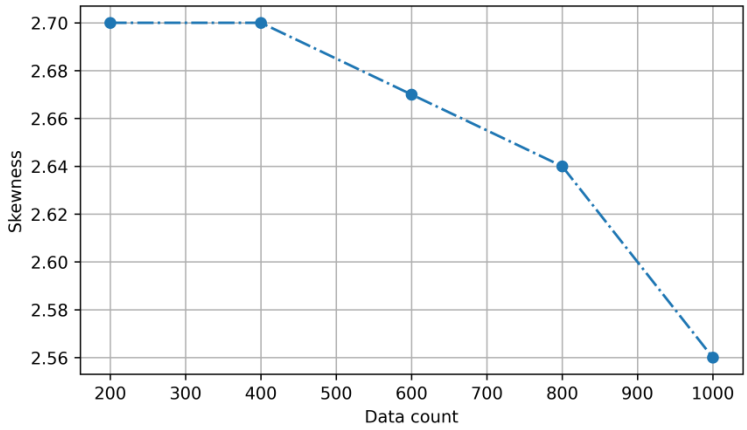

Figure 16: Skewness of the proposed system

The skewness of the proposed system for varying the number of input has been shown in figure 16. The skewness of the proposed system reducing theskewness by 2.56 when the number of imagesare increased and attains a maximum value of 2.70 when the number of images is reduced. The skewness of the proposed system has been decreased by using level check counter CNN that determine the additional and transitional lumbar vertebrae of the spinal cord.

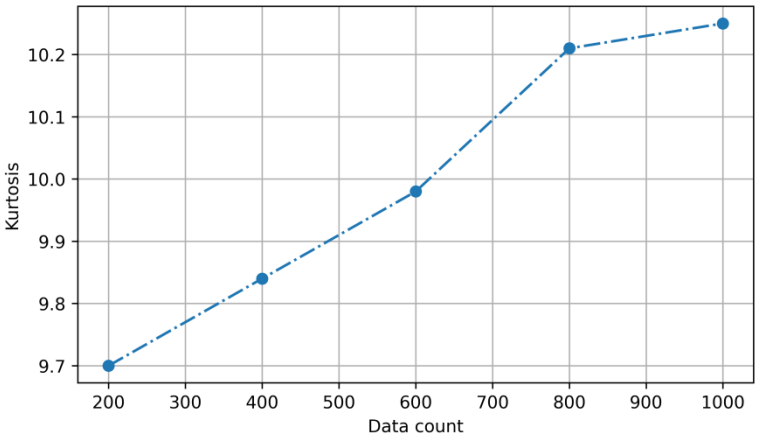

Figure17: Kurtosis of the proposed system

The kurthosis of the proposed system for varying the number of input has been shown in figure 17. The kurthosis of the proposed system achieved to increasing thekurthosis by 10.3 when the number of images are increased and attains a minimum value of 9.7 when the number of images is reduced. The kurthosis of the proposed system has been increased by using level check counter CNN that determine the additional and transitional lumbar vertebrae of the spinal cord.

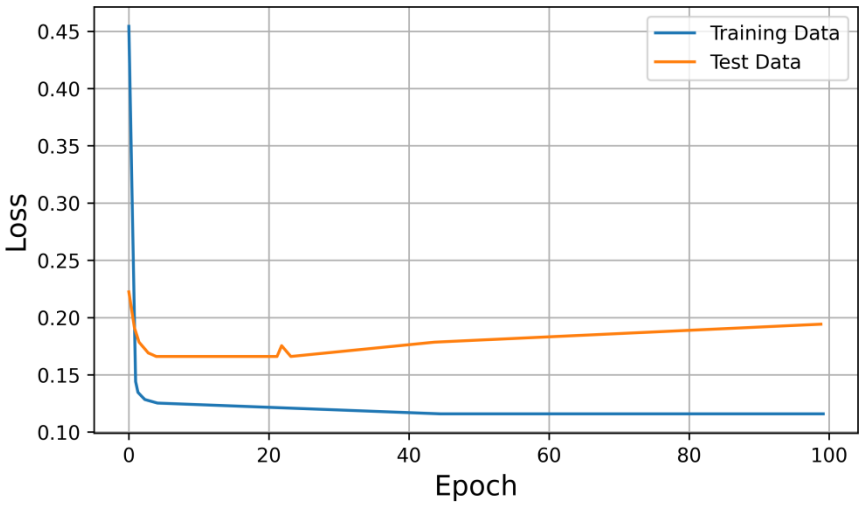

Figure 18: Loss of the proposed system

The loss of the proposed system for varying the number of input samples has been shown in figure 18. The training data of the proposed system achieves to reduce the loss value of 0.13 when the number of samples is increased and attains a maximum loss value of 0.45 when the number of images is reduced. The test data of the proposed system also has been reduced the loss value by 0.19 and increase the loss value 0.23 when is compared with the number of input data. Therefore the proposed system reduce the loss by using Visual bipartite matching loss feature transformer with extract the features such as cobb angle, area between anterior and posterior vertebra, end plate angle, local curvature, bone structure and intervertebral distance.

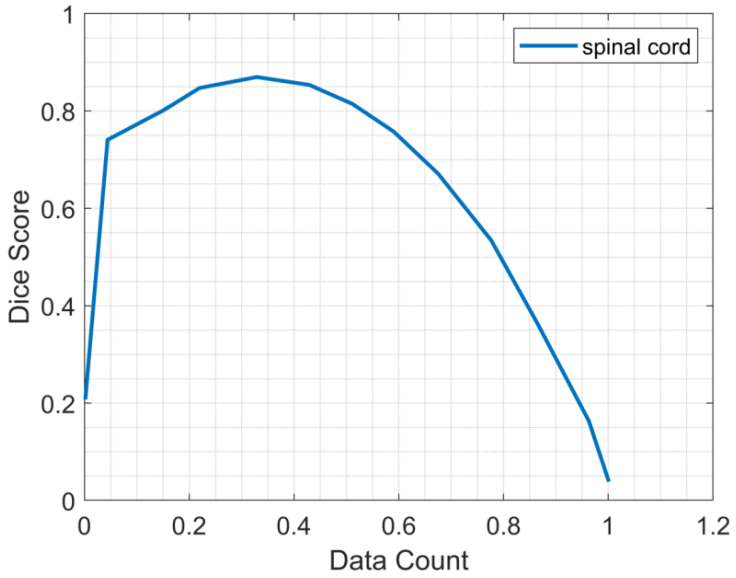

Figure 19: Dice score of the proposed system.

The dice score of the proposed system for varying the number of input samples has been shown in figure 19. The training data of the proposed system achieves to reduce the dice score of 0.1 when the number of samples is increased andattains a maximum dice score of 0.2 when the number of images is reduced. The test data of the proposed system also has been reduced the dice score by using the Multi-Atlas Instance SegNet to segment all localized images.

Comparison of Proposed model with Previous Models

This section emphasizes the effectiveness of the proposed model by comparing it with the outcomes of existing methodologies and illustrating their outcomes based on several metrics. The comparisons are made from the previous techniques with the various performance metrics such as accuracy, error, computational time, and FNR. Comparisons are made with the existing techniques such as CNN+RF, CNN+NN, CNN+Adaboost and CNN+LSTM [25].

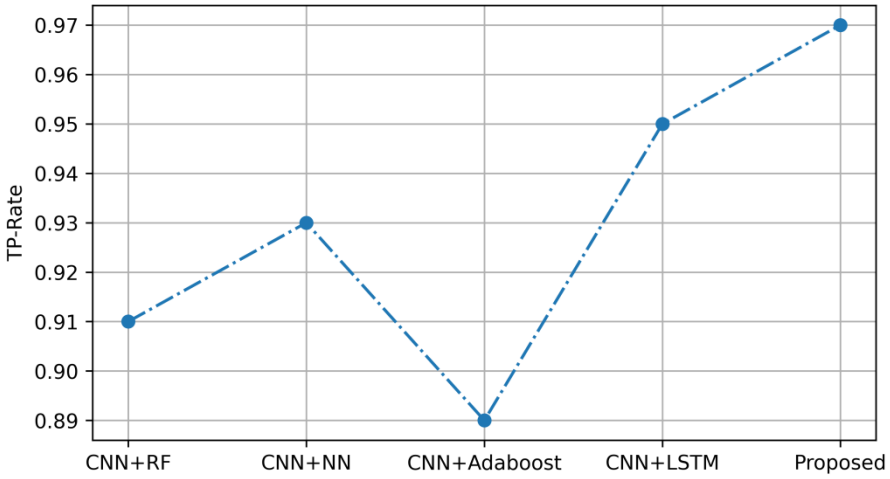

Figure 20: Comparison of TP-Rate

Figure 20 shows a comparison of the TP-rate of the proposed model with existing techniques such as CNN+RF, CNN+NN, CNN+Adaboost and CNN+LSTM whereas the proposed system attains a maximum TP-rate value by 0.97 when compared with the other techniques. The existing techniques such as CNN+RF, CNN+NN, CNN+Adaboost and CNN+LSTM are attains 0.91, 0.93, 0.89,0.95respectively. The proposed model has highTP-rate of 0.97 than existing models even though the numbers of images are increased. As a result, it is noticed that the proposed system has the highest TP-rate because of the novel technique Bilsky Phenotype grading classifier.

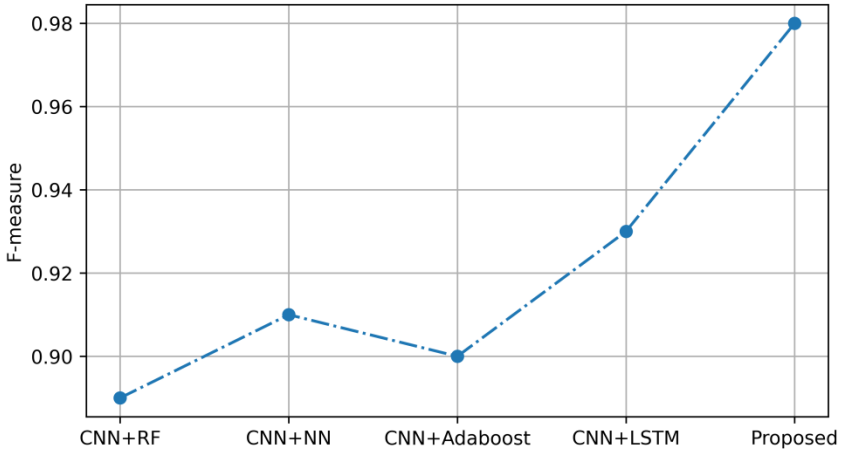

Figure 21: Comparison of the F-measure

Figure 21 shows a comparison of the F-measureof the proposed model with existing techniques such as CNN+RF, CNN+NN, CNN+Adaboost and CNN+LSTM whereas the proposed system attains a maximum F-measure value by 0.98 when compared with the other techniques. The existing techniques such as CNN+RF, CNN+NN, CNN+Adaboost and CNN+LSTM are attains 0.88, 0.91, 0.90,0.93respectively. The proposed model has highF-measure of 0.97 than existing models even though the numbers of images are increased. As a result, it is noticed that the proposed system has the highest F-measure because of the novel technique Bilsky Phenotype grading classifier.

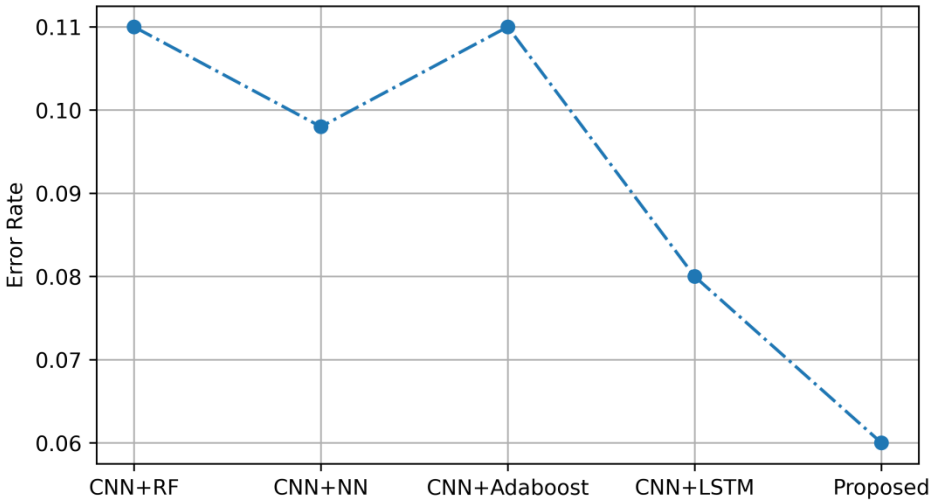

Figure 22: Comparison of error rate

Figure 22 shows a comparison of the error rate of the proposed model with existing techniques such as CNN+RF, CNN+NN, CNN+Adaboost and CNN+LSTM whereas the proposed system attains to reduce the error rate value by 0.06 when compared with the other techniques. The existing techniques such as CNN+RF, CNN+NN, CNN+Adaboost and CNN+LSTM are attains 0.11, 0.10, 0.11,0.08respectively. The proposed model has reduced the error rate of 0.06 than existing models even though the number of images are increased. As a result, it is noticed that the proposed system has the low error rate because of the novel technique circular anisotropic localization mechanism thereby eliminate localization error.

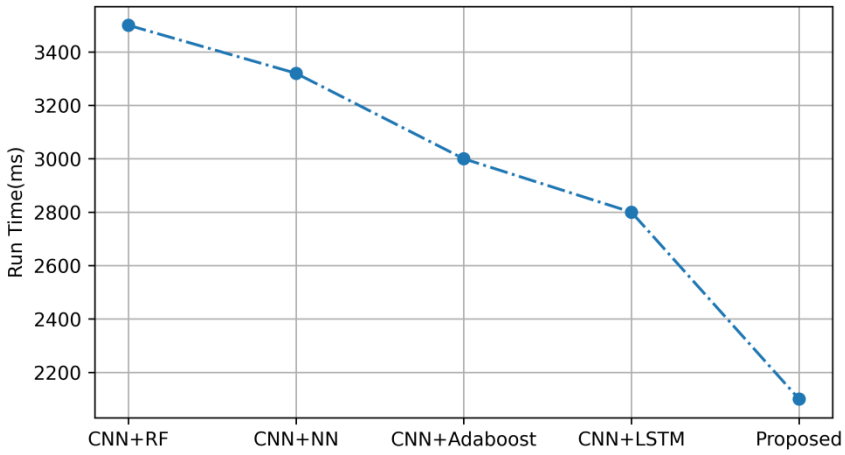

Figure 23: Comparison of the run time (ms)

Figure 23 shows a comparison of the error rate of the proposed model with existing techniques such as CNN+RF, CNN+NN, CNN+Adaboost and CNN+LSTM whereas the proposed system attains to reduce the error rate value by 2100ms when compared with the other techniques. The existing techniques such as CNN+RF, CNN+NN, CNN+Adaboost and CNN+LSTM are attains3500ms, 3300ms, 3000ms, 2800msrespectively. The proposed model has reduced the error rate of 2100ms than existing models even though the numbers of images are increased. As a result, it is noticed that the proposed system has the low error rate because of the novel technique Bilsky Phenotype grading classifier.

Overall, when compared with the existing techniques such as CNN+RF, CNN+NN, CNN+Adaboost and CNN+LSTM. The model proposed in this study has a very highTP-rate of 0.97%, low error of 0.06%, low computational time of 2100ms.

CONCLUSION

Pipelined Multilayer AI based point of care model has been presented in this research in which POCT based AI techniques were used to diagnosis the various spinal cord disorders in big clinical data such as spinal osteoarthritis, Lumbar Spinal Stenosis (LSS) and spinal deformities are the leading cause for back pain. Thus these techniques

provided quantitative segmentation accuracy evaluation results. Overall the proposed model provides low error rate and run time as 0.06% and 2100ms respectively. Circular anisotropic localization mechanism is used to properly localized all vertebrae of the spinal cord, which are that segmented by the techniques of Multi-Atlas Instance SegNet which provide smooth image details with high dice score by 0.2% in segmenting intervertebral disc, sagittal region, and spinal canal.BilskyPhenotype grading classifier is classified the various spinal cord disorders such as lumbar spinal stenosis, spinal deformities and spinal osteoarthritis without centroid detection thereby enhance the detection rate without misclassification. Hence the proposed AI based point of care model effectively diagnose various spinal cord disorders with its sublevels at an early stage with accurate labelling, segmentation and domineering feature extraction on the localized spinal cord components.When compared with the existing techniquessuch as CNN+RF, CNN+NN, CNN+Adaboost and CNN+LSTM, the proposed modelhas a high TP-rate and F-measure as 0.97%, 0.98% respectively.

REFERENCES

[1]. Damhorst, G.L., Tyburski, E.A., Brand, O., Martin, G.S. and Lam, W.A., 2019. Diagnosis of acute serious illness: the role of point-of-care technologies. Current opinion in biomedical engineering, 11, pp.22-34. https://doi.org/10.1016/j.cobme.2019.08.012

[2]. Olakotan, O.O. and Yusof, M.M., 2020. Evaluating the alert appropriateness of clinical decision support systems in supporting clinical workflow. Journal of biomedical informatics, 106, p.103453. https://doi.org/10.1016/j.jbi.2020.103453

[3]. Jain, S., Nehra, M., Kumar, R., Dilbaghi, N., Hu, T., Kumar, S., Kaushik, A. and Li, C.Z., 2021. Internet of medical things (IoMT)-integrated biosensors for point-of-care testing of infectious diseases. Biosensors and Bioelectronics, 179, p.113074. https://doi.org/10.1016/j.bios.2021.113074

[4]. Stranieri, A., Venkatraman, S., Minicz, J., Zarnegar, A., Firmin, S., Balasubramanian, V. and Jelinek, H.F., 2022. Emerging point of care devices and artificial intelligence: Prospects and challenges for public health. Smart Health, 24, p.100279. https://doi.org/10.1016/j.smhl.2022.100279

[5]. Kasparick, M., Andersen, B., Franke, S., Rockstroh, M., Golatowski, F., Timmermann, D., Ingenerf, J. and Neumuth, T., 2019. Enabling artificial intelligence in high acuity medical environments. Minimally Invasive Therapy & Allied Technologies, 28(2), pp.120-126. https://doi.org/10.1080/13645706.2019.1599957

[6]. Sakai, D., Schol, J. and Watanabe, M., 2022. Clinical Development of Regenerative Medicine Targeted for Intervertebral Disc Disease. Medicina, 58(2), p.267. https://doi.org/10.3390/medicina58020267

[7]. Kumar, V., Patel, S., Baburaj, V., Vardhan, A., Singh, P.K. and Vaishya, R., 2022. Current understanding on artificial intelligence and machine learning in orthopaedics–A scoping review. Journal of Orthopaedics. https://doi.org/10.1016/j.jor.2022.08.020

[8]. Durand, W.M., Lafage, R., Hamilton, D.K., Passias, P.G., Kim, H.J., Protopsaltis, T., Lafage, V., Smith, J.S., Shaffrey, C., Gupta, M. and Kelly, M.P., 2021. Artificial intelligence clustering of adult spinal deformity sagittal plane morphology predicts surgical characteristics, alignment, and outcomes. European Spine Journal, 30(8), pp.2157-2166. https://doi.org/10.1007/s00586-021-06799-z

[9]. Nuwer, M.R., MacDonald, D.B. and Gertsch, J., 2022. Monitoring scoliosis and other spinal deformity surgeries. In Handbook of Clinical Neurology (Vol. 186, pp. 179-204). Elsevier. https://doi.org/10.1016/B978-0-12-819826-1.00014-4

[10]. Saravi, B., Hassel, F., Ülkümen, S., Zink, A., Shavlokhova, V., Couillard-Despres, S., Boeker, M., Obid, P. and Lang, G.M., 2022. Artificial intelligence-driven prediction modeling and decision making in spine surgery using hybrid machine learning models. Journal of Personalized Medicine, 12(4), p.509. https://doi.org/10.3390/jpm12040509

[11]. Mourad, R., Kolisnyk, S., Baiun, Y., Falk, A., Yuriy, T., Valerii, F., Kopeev, A., Suldina, O., Pospelov, A., Kim, J. and Rusakov, A., 2022. Performance of hybrid artificial intelligence in determining candidacy for lumbar stenosis surgery. European Spine Journal, 31(8), pp.2149-2155. https://doi.org/10.1007/s00586-021-06799-z

[12]. Culbert, M.P., Warren, J.P., Dixon, A.R., Fermor, H.L., Beales, P.A. and Wilcox, R.K., 2022. Evaluation of injectable nucleus augmentation materials for the treatment of intervertebral disc degeneration. Biomaterials Science. 10.1039/d1bm01589c

[13]. Liang, H., Luo, R., Li, G., Zhang, W., Song, Y. and Yang, C., 2022. The Proteolysis of ECM in Intervertebral Disc Degeneration. International Journal of Molecular Sciences, 23(3), p.1715. https://doi.org/10.3390/ijms23031715

[14]. Hallinan, J.T.P.D., Zhu, L., Zhang, W., Kuah, T., Lim, D.S.W., Low, X.Z., Cheng, A.J., Eide, S.E., Ong, H.Y., Muhamat Nor, F.E. and Alsooreti, A.M., 2022. Deep Learning Model for Grading Metastatic Epidural Spinal Cord Compression on Staging CT. Cancers, 14(13), p.3219. https://doi.org/10.3390/cancers14133219

[15]. Tang, H., Pei, X., Huang, S., Li, X. and Liu, C., 2020. Automatic lumbar spinal CT image segmentation with a dual densely connected U-Net. IEEE Access, 8, pp.89228-89238. 10.1109/ACCESS.2020.2993867

[16]. Zhang, X., Li, Y., Liu, Y., Tang, S.X., Liu, X., Punithakumar, K. and Shi, D., 2021. Automatic spinal cord segmentation from axial-view MRI slices using CNN with grayscale regularized active contour propagation. Computers in Biology and Medicine, 132, p.104345. https://doi.org/10.1016/j.compbiomed.2021.104345

[17]. Al-Kafri, A.S., Sudirman, S., Hussain, A., Al-Jumeily, D., Natalia, F., Meidia, H., Afriliana, N., Al-Rashdan, W., Bashtawi, M. and Al-Jumaily, M., 2019. Boundary delineation of MRI images for lumbar spinal stenosis detection through semantic segmentation using deep neural networks. IEEE Access, 7, pp.43487-43501. 10.1109/ACCESS.2019.2908002

[18]. Mushtaq, M., Akram, M.U., Alghamdi, N.S., Fatima, J. and Masood, R.F., 2022. Localization and Edge-Based Segmentation of Lumbar Spine Vertebrae to Identify the Deformities Using Deep Learning Models. Sensors, 22(4), p.1547. https://doi.org/10.3390/s22041547

[19]. Chae, D.S., Nguyen, T.P., Park, S.J., Kang, K.Y., Won, C. and Yoon, J., 2020. Decentralized convolutional neural network for evaluating spinal deformity with spinopelvic parameters. Computer Methods and Programs in Biomedicine, 197, p.105699. https://doi.org/10.1007/s00586-021-06799-z

[20]. Rehman, F., Shah, S.I.A., Riaz, N. and Gilani, S.O., 2019. A robust scheme of vertebrae segmentation for medical diagnosis. IEEE Access, 7, pp.120387-120398. 10.1109/ACCESS.2019.2936492

[21]. Zhang, J., Cheuk, K.Y., Xu, L., Wang, Y., Feng, Z., Sit, T., Cheng, K.L., Nepotchatykh, E., Lam, T.P., Liu, Z. and Hung, A.L., 2020. A validated composite model to predict risk of curve progression in adolescent idiopathic scoliosis. EClinicalMedicine, 18, p.100236. https://doi.org/10.1016/j.eclinm.2019.12.006

[22]. Ahammad, S.H., Rajesh, V. and Rahman, M.Z.U., 2019. Fast and accurate feature extraction-based segmentation framework for spinal cord injury severity classification. IEEE Access, 7, pp.46092-46103. 10.1109/ACCESS.2019.2909583

[23]. B. Glocker, D. Zikic, E. Konukoglu, D.R. Haynor, A. Criminisi Vertebrae Localization in Pathological Spine CT via Dense Classification from Sparse AnnotationsInternational Conference on Medical Image Computing and Computer Assisted Intervention (MICCAI), Nagoya, Japan, September 2013. https://doi.org/10.1007/978-3-642-40763-5_33

[24]. B. Glocker, J. Feulner, A. Criminisi, D.R. Haynor, E. Konukoglu Automatic Localization and Identification of Vertebrae in Arbitrary Field-of-View CT ScansInternational Conference on Medical Image Computing and Computer Assisted Intervention (MICCAI), Nice, France, October 2012

[25]. Ahammad, S.H., Rajesh, V., Rahman, M.Z.U. and Lay-Ekuakille, A., 2020. A hybrid CNN-based segmentation and boosting classifier for real time sensor spinal cord injury data. IEEE Sensors Journal, 20(17), pp.10092-10101. 10.1109/JSEN.2020.2992879

[26]. Aarabi, B., Chixiang, C., Simard, J.M., Chryssikos, T., Stokum, J.A., Sansur, C.A., Crandall, K.M., Olexa, J., Oliver, J., Meister, M.R. and Cannarsa, G., 2022. Proposal of a Management Algorithm to Predict the Need for Expansion Duraplasty in American Spinal Injury Association Impairment Scale Grades A–C Traumatic Cervical Spinal Cord Injury Patients. Journal of neurotrauma, 39(23-24), pp.1716-1726. https://doi.org/10.1089/neu.2022.0218